International Immunopharmacology 75 (2019) 105751

Contents lists available at ScienceDirect

International Immunopharmacology

journal homepage: www.elsevier.com/locate/intimp

Short communication

# Combination of acute intravenous methamphetamine injection and LPS challenge facilitate leukocyte infiltration into the central nervous system of C57BL/6 mice

Daniela DiCaro[a], Hiu Ham Lee[a], Christian Belisario[a], Raddy L. Ramos[a], Luis R. Martinez[a,b,*]

[a] Department of Biomedical Sciences, NYIT College of Osteopathic Medicine, New York Institute of Technology, Old Westbury, NY, USA
[b] Department of Biological Sciences, The Border Biomedical Research Center, The University of Texas at El Paso, TX, USA

ARTICLE INFO

*Keywords:*
Cytokines
Inflammation
Macrophages
Methamphetamine
Neutrophils

ABSTRACT

Methamphetamine (METH) is a stimulant of the central nervous system (CNS) that causes behavioral changes in users. METH is slowly cleared from brain tissue and its chronic use is neurotoxic. METH also alters the cellular and chemical components of inflammation. However, little is known about the effect of a single intravenous dose of METH followed by bacterial lipopolysaccharide (LPS) injection on cellular infiltration and cytokine release in brain tissue. Using a murine model of acute METH administration and flow cytometry, we found that combination of METH and LPS stimulate the infiltration of macrophages ($F4/80^{+}$ cells) and neutrophils ($Ly\text{-}6G^{+}$ cells) into the CNS. Histological sections of the brainstem of METH-treated and LPS-challenged C57BL/6 mice demonstrated considerable leukocyte infiltration relative to untreated, LPS, and METH groups. Moreover, rodents treated with LPS alone or combined with METH showed elevated levels of pro-inflammatory cytokines mRNA in brain tissue. Our observations are important because recognizing neuroinflammatory changes after acute METH administration might help us to understand METH-induced neurotoxicity in users.

## 1. Introduction

Methamphetamine (METH) is an extremely addictive illicit drug that acts as a powerful central nervous system (CNS) stimulant and its abuse is a rising public health concern worldwide [1]. In 2015, a survey by the United States (US) Department of Health and Human Services revealed that about 897,000 people aged 12 or older were current users of METH [2]. The same year, nearly 6000 people died from stimulant use, mostly METH, a 255% increase from 2005, according to the US Centers for Disease Control and Prevention [3]. The 2017 World Drug Report by the United Nations Office on Drugs and Crime published that the prevalence of the use of METH and other amphetamines was approximately 37 million people worldwide [4]. In the US, 11% of deaths associated with drug overdose are attributed to METH and other stimulants [3].

Intravenous METH injection is a common route of abuse, allowing the user to feel the euphoric effects within minutes due to the release of dopamine [5]. METH abuse is neurotoxic due to its slow clearance [6] and can cause hyperthermia or increased brain temperatures, which can cause aberrant neural function such as irregular neurotransmitter release and oxidative stress [7]. Brain hyperthermia can also cause an increase in the permeability of the blood-brain barrier leading to brain edema that induces brain cell injury or death [8]. METH also acts on immune cells, diminishing the effector functions of monocytes, natural killer cells, dendritic cells, macrophages, and neutrophils [9–11]. For example, METH impairs leukocyte migration, phagocytosis, and microbicidal activity [12]. Furthermore, METH use is associated with an increased risk of contracting infectious diseases including HIV, Hepatitis C, cutaneous bacterial infections, and sexually transmitted diseases [1,13].

In this study, we investigated the effect of acute METH administration on the inflammatory response in murine brain tissue after antigenic challenge. We selected lipopolysaccharide (LPS), a component of the cell wall of gram-negative bacteria, for these studies because which is a T-cell independent antigen that can induce a strong immune response in rodents. Our data demonstrate that combination of acute METH and LPS injection stimulates cellular infiltration into the CNS of mice. While LPS treatment alone was responsible for increased levels of pro-inflammatory cytokines in brain tissue. Our observations are important because the identification of neuroinflammatory changes in the

* Corresponding author at: The University of Texas at El Paso, College of Science, The Border Biomedical Research Center, Department of Biological Sciences, 500 W., University Ave., Bioscience Research Building, Room 2.170, El Paso, TX 79968, USA.
*E-mail address:* lmartinez43@utep.edu (L.R. Martinez).

https://doi.org/10.1016/j.intimp.2019.105751
Received 15 June 2019; Accepted 9 July 2019
Available online 15 July 2019

brain after acute METH exposure may shed light on the mechanisms of METH-induced neurotoxicity.

## 2. Materials and methods

### 2.1. Mouse model of acute METH administration

To simulate an acute usage of METH, C57BL/6 mice ($n = 5$ per group; age 6–8 weeks; male and female; Charles Rivers) were injected through the tail vein with a 100 mL suspension of phosphate buffer saline (PBS; untreated negative control), 5 mg/kg METH (Sigma), 5 mg/kg LPS (Sigma), or combination of METH and LPS (METH + LPS). Four hours after injections, animals were euthanized using $CO_2$, their brains excised using aseptic techniques, and the tissue used to determine cellular infiltration, immunohistochemistry, and gene expression studies. We selected this time point (4 h) because we were interested in understanding early inflammatory responses to a single injection of METH, LPS, or combination.

### 2.2. Ethics statement

All animal studies were conducted according to the experimental practices and standards approved by the Institutional Animal Care and Use Committee at the NYIT College of Osteopathic Medicine (NYIT COM) (Protocol #: 2016-LRM-01).

### 2.3. Rationale for METH doses used in mice

The concentrations of METH used in the experiments are physiologically relevant. Controlled studies have indicated that a single 260 mg dose peaks at a level of 7.5 μM [14]. Thus, a single dose of 260 mg would be expected to produce 7.5 to 28.8 μM blood METH levels. Therefore, we selected 5 mg/kg/day to perform our *in vivo* experiments [10,12,15,16]. Additionally, the dose of METH utilized to perform these experiments is within the range dose (4 to 8 mg/kg/day) used in a recent study investigating the effects of chronic METH administration on brain structure and function in rodents [17].

### 2.4. Flow cytometry analysis

For flow cytometry staining, primary cells were isolated from 0.1 g of excised and homogenized brain tissue in 1 mL PBS from 5 mice treated with PBS, LPS, METH, and METH + LPS as described above; the cells were washed and then stained with fluorescence-labeled antibodies. Anti-F4/80 (macrophages; dilution: 1:1000; Invitrogen) or Ly-6G (neutrophils; dilution: 1:1000; Leinco Technologies)-FITC and their corresponding isotype controls were purchased (Becton Dickinson). Samples were processed on a BD Accuri C6 flow cytometer and were analyzed using the FCS express software version 4.

### 2.5. Histology

After METH administration, each mouse was euthanized and vascularly perfused with 4% paraformaldehyde (PFA) and 10% sucrose solutions in PBS (pH 7.4). Then, brains were excised and fixed in 4% PFA for 24 h. Brainstem tissues were processed, embedded in paraffin, and 4 μm sagittal sections were fixed to glass slides. The tissues were then stained for either neutrophils or macrophages using Ly-6G antibody (dilution: 1:1000; Leinco Technologies) or F4/80 antibody (dilution: 1:1000; Invitrogen), respectively. Slides were visualized using an Olympus BX41 inverted microscope (Olympus) and images were acquired with an Olympus DP70 camera using Olympus DP Controller software version 3. Quantitative measurements of individual image intensities in the histological analyses for Ly-6G$^+$ and F4/80$^+$ cells were performed using ImageJ software (National Institutes of Health).

### 2.6. RNA extraction and cDNA synthesis

For RNA extraction, brain tissue was flash frozen in liquid nitrogen then pulverized using a glass tissue grinder (Wheaton). TRIzol reagent (Thermofisher) was added to resulting tissue particulate and RNA extraction was performed using the Purelink RNA Mini Kit (Thermofisher), following the manufacturer's instructions. To remove any genomic DNA carryover, the samples were treated with DNase I (Qiagen) for 30 min at 37 °C, followed by heat inactivation for 5 min at 65 °C. Then, 1 μg of total RNA was used to synthesize cDNA with the Bio-Rad iScript reverse transcriptase kit (Bio-Rad), following the manufacturer's instructions. The control reaction was set up using all components of the reaction mixture but without the reverse transcriptase enzyme (*i.e.*, no reverse transcriptase).

### 2.7. Real-time polymerase chain reaction (RT-PCR)

The primers used for RT-PCR analysis were as follows: Sequences of primers were as follows: IL-1α (forward, 5′-CGCTTGAGTCGGCAAAGAAATC′3′; reverse, 5′-GTGCAAGTCTCATGAAGTGAGC-3′), IL-1β (forward, 5′-TGCCACCTTTTGACAGTGATG-3′; reverse, 5′-ATGAGTGATACTGCCTGCCTG-3′), IL-6 (forward, 5′-GAGAGGAGACTTCACAGAGGATACC-3′; reverse, 5′-GAATTGCCATTGCACAACTCTTTTC-3′), KC (forward, 5′-GGCGCCTATCGCCAATGAG-3′; reverse, 5′-GTGTGGCTATGACTTCGGTTTG-3′), MIP-2 (forward, 5′-TGAACAAAGGCAAGGCTAACTG-3′; reverse, 5′-GTGTGGCTATGACTTCGGTTTG-3′), and TNF-α (forward, 5′-GCCTCTTCTCATTCCTGCTTG-3′; reverse, 5′-CTGATGAGAGGGAGGCCATT-3′). The efficiency of each primer was tested by using a 10-fold serial dilution of the cDNA mixture, and only primers with efficiencies between 95% and 105% were used for the analysis. The expression of genes was determined by quantitative PCR using iQ SYBR Green Supermix (Bio-Rad). Two different control reactions were included in the analysis, *i.e.*, a no-template control and a no reverse transcriptase control. We used actin rRNA as the reference gene (forward, 5′-CAGCTCGTGTCGTGAGATGT-3′; reverse, 5′-CGTAAGGGCCATGATGACTT-3′). Relative expression was determined using the cycle threshold (ΔΔCT) method on a Mastercycler RealPlex2 system (Eppendorf). Reactions were set up using 300 nM primers and 5 μL of the cDNA template (diluted 1:10). The cycling conditions used were as follows: 55 °C for 30 min and then 40 amplification cycles of 95 °C for 15 s, 55 °C for 30 s, and 72 °C for 30 s. The samples were cooled to 55 °C, and a melting curve for temperatures between 55 °C and 95 °C, with 0.5 °C increments, was recorded. All reactions were carried out in triplicate. Target gene expression was measured using expression relative to that of the actin reference gene. Data analysis was carried out using Mastercycler ep realplex software version 2.0 (Eppendorf).

### 2.8. Statistical analysis

All data were subjected to statistical analysis using GraphPad Prism 7.0 (GraphPad Software). $P$ values for multiple comparisons were calculated by analysis of variance (ANOVA) and were adjusted by use of the Tukey post-hoc analysis. $P$ values of $< 0.05$ were considered significantly.

## 3. Results

### 3.1. Combination of METH and LPS enhances leukocyte infiltration to the brain

We assessed the infiltration of leukocytes into the brain of C57BL/6 mice after acute METH administration and LPS challenge using flow cytometry (Figs. 1 and 2). We did not observe any cellular differences in mice treated with PBS, LPS or METH alone. However, brain tissue of METH + LPS-treated animals resulted in significant infiltration of neutrophils (Ly-6G$^+$; $P < 0.001$, untreated, METH, and LPS)

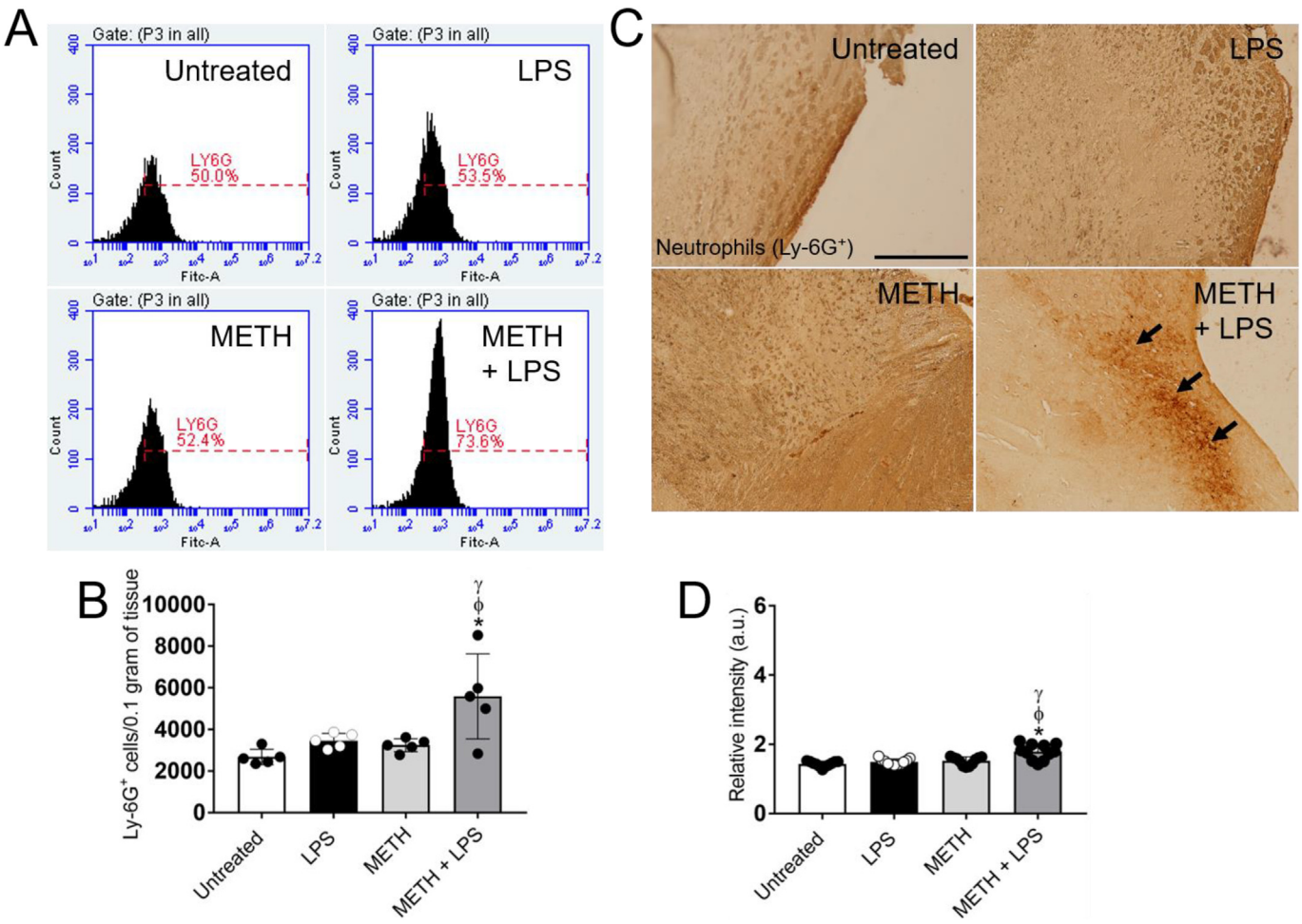


**Fig. 1.** Combination of METH and LPS challenge increase neutrophil infiltration to the brain. (A) Representative plots of Ly-6G$^+$ cells in brain tissue excised from untreated, LPS, METH and METH + LPS-injected C57BL/6 mice were analyzed by flow cytometry. Each plot was generated after 0.1 g of tissue was analyzed. (B) Counts of neutrophils (Ly-6G$^+$) per 0.1 g of brain tissue of C57BL/6 mice ($n$ = 5) 4 h post-METH and LPS administration are shown. Bars indicate the average number of Ly-6G$^{\pm}$ cells (each circle represents 0.1 g of brain tissue homogenates per mouse; $n$ = 5) for each experimental condition, and error bars indicate standard deviation (STDEV). (C) Representative Ly-6G stained sections of brainstem tissue excised from untreated, LPS, METH and METH + LPS-injected animals are shown (scale bar, 500 μm; 40× magnification) with brown staining (black arrows) indicating cellular infiltration. (D) The relative intensity of Ly-6G$^{\pm}$ cells was quantified using NIH ImageJ software. Bars indicate the average relative intensity (arbitrary units, a. u.; each circle represents a random area of the field; $n$ = 10) for each experimental condition, and error bars indicate STDEV. For B and D, symbols (*, ϕ, and γ) indicate $P$ value significance ($P < 0.001$) calculated using analysis of variance (ANOVA) and adjusted by use of the Tukey post-hoc analysis. *, ϕ, and γ indicate significantly higher Ly-6G$^+$ cell infiltration than in the untreated, LPS, and METH-treated groups, respectively. These experiments were performed twice and similar results were obtained. (For interpretation of the references to color in this figure legend, the reader is referred to the web version of this article.)

(Fig. 1A–B) and macrophages (F4/80$^+$; $P < 0.001$, untreated, METH, and LPS) (Fig. 2A–B). Immunohistochemistry analyses of the brainstem also revealed notable inflammatory differences between METH + LPS-treated mice and animals of the other groups (Figs. 1C–D and 2C–D). The images of tissue sections of brains excised from METH + LPS-treated animals displayed considerable infiltration (black arrows; brown staining) of neutrophils (Fig. 1C) and macrophages (Fig. 2C), therefore, validating the flow cytometry analyses. Moreover, the intensity of leukocyte infiltration was quantified and demonstrated that rodents treated with METH + LPS exhibited significant infiltration of neutrophils (Fig. 1D) and macrophages (Fig. 2D) relative to the untreated ($P < 0.001$), LPS ($P < 0.001$), and METH ($P < 0.001$) groups. Together, we concluded that acute METH injection and LPS challenge enhances infiltration of phagocytic cells into the CNS.

### 3.2. LPS stimulates pro-inflammatory cytokines production in vivo

We investigated the role of METH, LPS, or combination on the gene expression of pro-inflammatory cytokines in the brain (Fig. 3). Using RT-PCR, we quantified the mRNA expression levels of the pro-inflammatory cytokines, IL-1α, IL-1β, IL-6, KC, MIP-2, and TNF-α, in brain tissue 4 h after METH administration and LPS challenge. Our findings showed significant expression levels of IL-1α, IL-1β, IL-6, KC, MIP-2, and TNF-α in cerebral tissue of LPS-challenged animals compared to the untreated and METH-treated groups ($P < 0.05$). Given that the expression of cytokine genes in mice treated with METH + LPS were similar (IL-1α, IL-6, KC, TNF-α) or evinced a similar trend (IL-1β, MIP-2) than those of animals treated with LPS and METH-treated mice had low levels of pro-inflammatory cytokines expression, we concluded that LPS not METH was responsible for stimulating cytokine production *in vivo*.

## 4. Discussion

METH is a worldwide healthcare burden causing detrimental effects on the brain of users due to its slow clearance from the CNS [6]. We investigated the role of METH and LPS challenge on neuroinflammation *in vivo* after acute administration. Our findings show that an acute

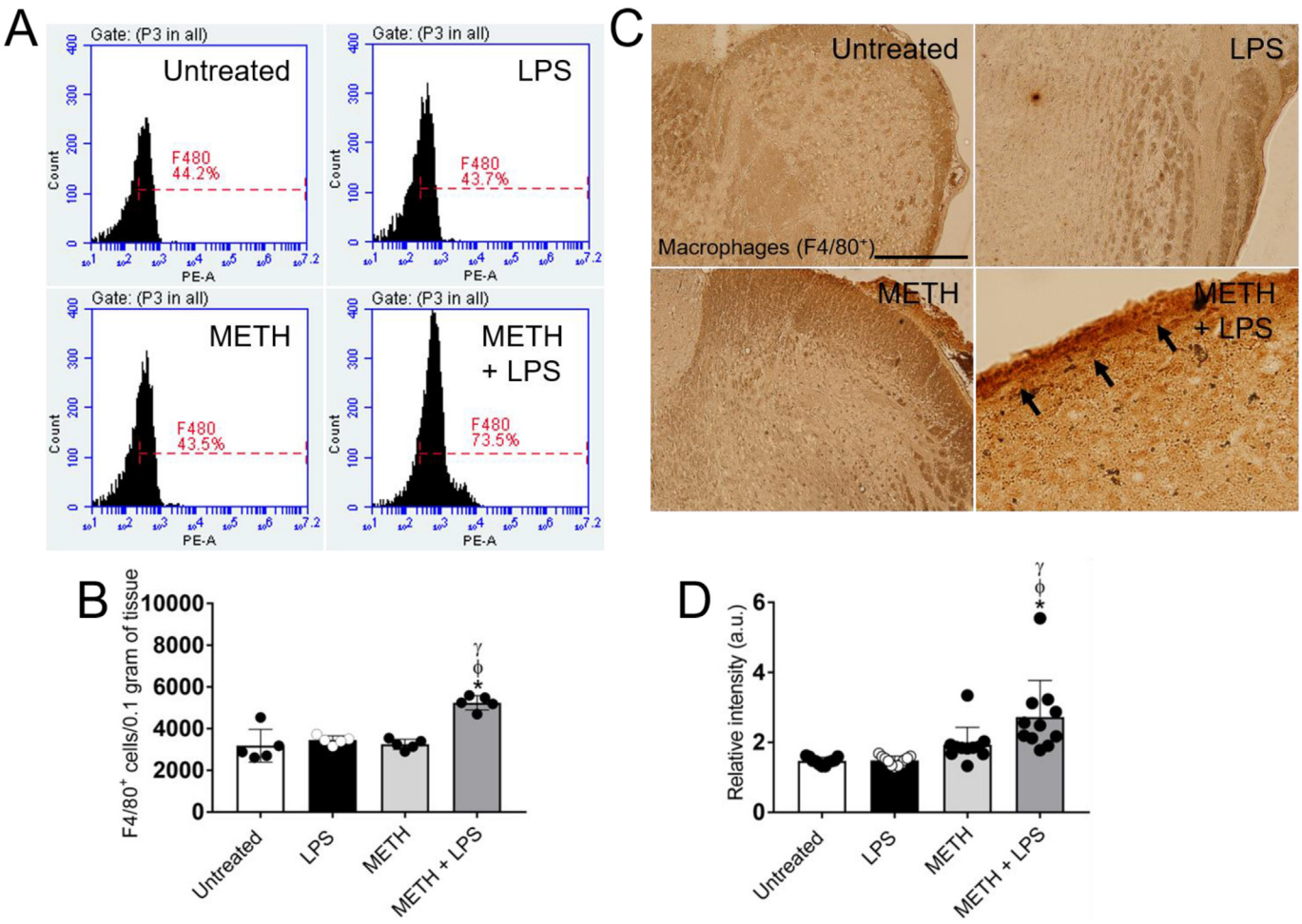


**Fig. 2.** Combination of METH and LPS challenge increase macrophage infiltration to the brain. (A) Representative plots of F4/80$^+$ cells in brain tissue excised from untreated, LPS, METH and METH + LPS-injected C57BL/6 mice were analyzed by flow cytometry. Each plot was generated after 0.1 g of tissue was analyzed. (B) Counts of macrophages (F4/80$^+$) per 0.1 g of brain tissue of C57BL/6 mice ($n = 5$) 4 h post-METH and LPS administration are shown. Bars indicate the average number of F4/80$^{\pm}$ cells (each circle represents 0.1 g of brain tissue homogenates per mouse; $n = 5$) for each experimental condition, and error bars indicate STDEV. (C) Representative F4/80 stained sections of brainstem tissue excised from untreated, LPS, METH and METH + LPS-injected animals are shown (scale bar, 500 μm; 40× magnification) with brown staining (black arrows) indicating cellular infiltration. (D) The relative intensity of F4/80$^{\pm}$ cells was quantified using NIH ImageJ software. Bars indicate the average relative intensity (a. u.; each circle represents a random area of the field; $n = 10$) for each experimental condition, and error bars indicate STDEV. For B and D, symbols (*, ϕ, and γ) indicate $P$ value significance ($P < 0.001$) calculated using ANOVA and adjusted by use of the Tukey post-hoc analysis. *, ϕ, and γ indicate significantly higher F4/80$^+$ cell infiltration than in the untreated, LPS, and METH-treated groups, respectively. These experiments were performed twice and similar results were obtained. (For interpretation of the references to color in this figure legend, the reader is referred to the web version of this article.)

METH exposure and LPS challenge increase the infiltration of neutrophils and macrophages within the mouse brain. METH disrupts the blood brain barrier resulting in increased permeability and enabling the migration of monocytes [18]. The presence of leukocytes in the brain can have serious clinical implications resulting in neurotoxicity due to abundant release of reactive oxygen species (ROS) and inflammatory mediators. For example, METH-treated macrophages can be toxic to neurons by stimulating the release of nitric oxide and pro-inflammatory cytokines [19]. In this regard, we found high levels of TNF-α which has a direct effect on the expression of inducible nitric oxide synthase, the enzyme that catalyzes the production of nitric oxide through oxidation of l-arginine on the cytosolic side of the phagosome membrane [20]. Similarly, neurodegeneration of the substantia nigra involves the infiltration of macrophage/microglia cells [21]. Additionally, neutrophils moving across a layer of cerebrovascular endothelium can produce ROS, secrete proteases, and de-condensed DNA, promoting neurotoxicity [22]. We observed increased levels of KC and MIP-2 mRNA in brain tissue of METH + LPS-treated mice [23] and these cytokines stimulate neutrophil infiltration and support this hypothesis.

Since LPS combined with METH are required for phagocytic cell infiltration into brain tissue, this observation suggests that METH users that acquire a gram-negative bacterial infection may be particularly susceptible to leukocyte-induced neurotoxicity. This is especially of interest for future studies because METH injection is also associated with the introduction of bacteria into the skin, specifically if the user fails to clean injection sites or shares drug paraphernalia [24]. Furthermore, METH use causes formication, a sensation of something crawling on the body or under the skin, which can lead to skin-picking behavior and skin breakdown allowing infection by microorganisms [25].

We found that LPS, not METH, stimulates the production of pro-inflammatory cytokines after acute administration of the drug. Subcutaneous injection of LPS attenuates METH-induced striatal production of pro-inflammatory cytokines [26]. Although many studies support METH-induced dysregulation of pro-inflammatory cytokines in the CNS [26–28], it is conceivable that in our studies there was not sufficient time required for this substance of abuse to modulate the production of these immune mediators. Even though Gonçalves et al.

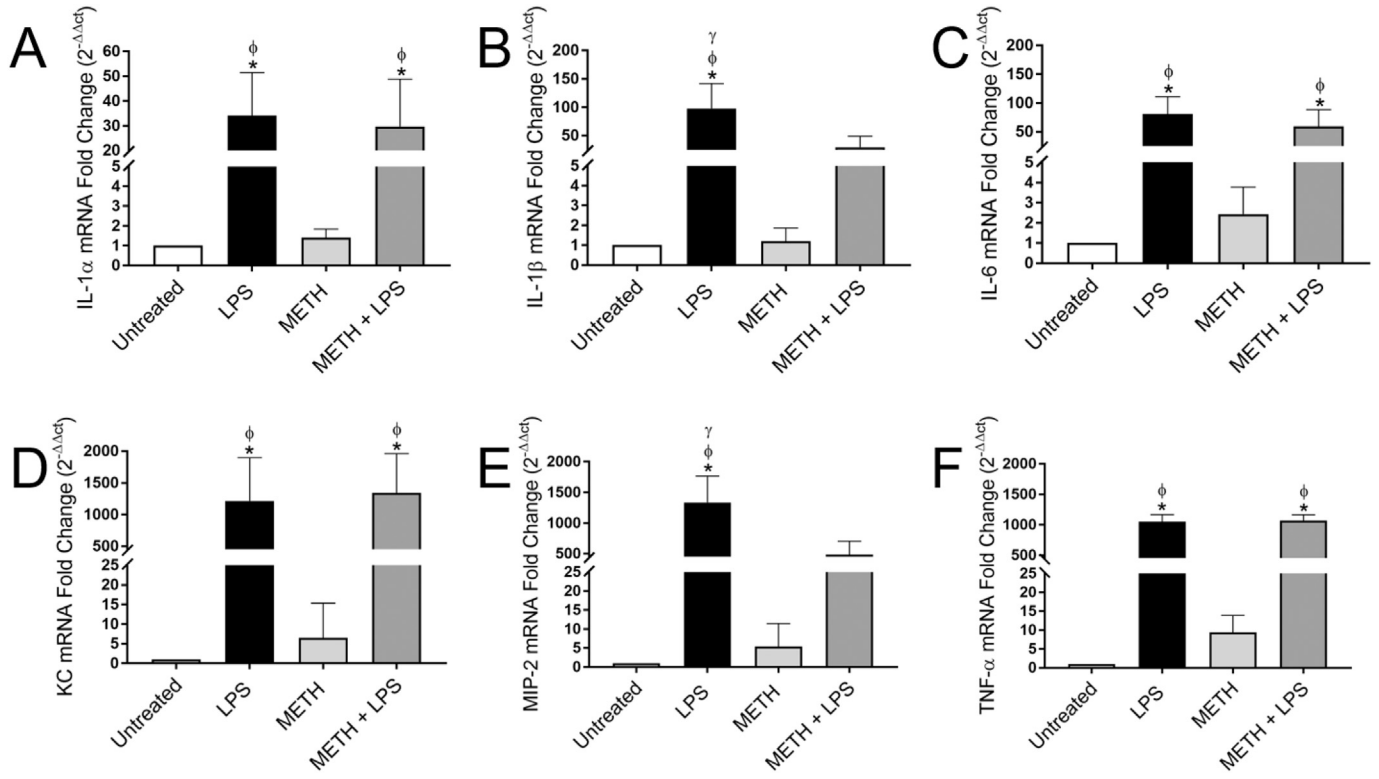


**Fig. 3.** Change in IL-1α (A), IL-1β (B), IL-6 (C), KC (D), MIP-2 (E), and TNF-α (F) gene expression in C57BL/6 mice brain 4 h post-METH injection. Relative expression was normalized to the housekeeping gene actin. Bars signify the average for each experimental condition ($n = 5$), and error bars indicate STDEV. Symbols (*, ϕ, γ) denote *P*-value significance ($P < 0.05$) calculated using ANOVA and adjusted by use of the Tukey post-hoc analysis. *, ϕ, γ represents significant increase in gene expression compared to the untreated, METH, or METH + LPS groups, respectively. These experiments were performed twice and similar results were obtained.

demonstrated that acute intraperitoneal administration of METH enhances production of IL-6 and TNF-α mRNA but not IL-L1β in the hippocampus, striatum, and frontal cortex in a time-lapse of 2 h [29], it is difficult to compare their study with ours given that the routes of METH administration used were different. Additionally, the discrepancies between both studies are amplified by the fact that they used older C57BL/6 mice (32 weeks), animals were treated with a single dose of METH six times higher than ours, and LPS was not used in combination with METH.

In conclusion, we demonstrated that acute METH and LPS intravenous administration increase the infiltration of macrophages and neutrophils into the brain of rodents. METH did not alter pro-inflammatory cytokine mRNA expression in the CNS. This short report provides insight into the regulatory activity of METH and LPS on the inflammatory response in brain tissue, which may have significant clinical implications in METH users.

## Declaration of Competing Interest

The authors declare no conflict of interest.

## Acknowledgements

D.D. was partially supported by the NYIT COM summer research program. C.B. was partially supported by the NYIT COM Academic Scholar program. R.L.R. and L.R.M. were supported by the National Institute of General Medical Sciences of the US National Institutes of Health (NIH) under award number 1R15GM117501-01A1. L.R.M. is funded and has an appointment in the Infectious Diseases and Immunology cluster of the Border Biomedical Research Center (BBRC; National Institute on Minority Health and Health Disparities award number 2G12MD007592), UTEP's Research Centers in Minority Institutions Program.

## Authorship

All authors contributed to the project design and experimental procedures, analyzed data, provided the figure presentation, and manuscript writing.

## References

[1] S.A. Salamanca, E.E. Sorrentino, J.D. Nosanchuk, L.R. Martinez, Impact of methamphetamine on infection and immunity, Front. Neurosci. 8 (2014) 445.
[2] Key Substance Use and Mental Health Indicators in the United States: Results From the 2015 National Survey on Drug Use and Health, (2015).
[3] F. Robles, Meth, the Forgotten Killer, Is Back. And It's Everywhere, The New York Times, 2018.
[4] World Drug Report United Nations Office on Drugs and Crime (2017).
[5] C.L. Hart, E.W. Gunderson, A. Perez, M.G. Kirkpatrick, A. Thurmond, S.D. Comer, R.W. Foltin, Acute physiological and behavioral effects of intranasal methamphetamine in humans, Neuropsychopharmacology 33 (8) (2008) 1847–1855.
[6] N.D. Volkow, J.S. Fowler, G.J. Wang, E. Shumay, F. Telang, P.K. Thanos, D. Alexoff, Distribution and pharmacokinetics of methamphetamine in the human body: clinical implications, PLoS One 5 (12) (2010) e15269.
[7] P.L. Brown, R.A. Wise, E.A. Kiyatkin, Brain hyperthermia is induced by methamphetamine and exacerbated by social interaction, J. Neurosci. 23 (9) (2003) 3924–3929.
[8] E. A. Kiyatkin, H. S. Sharma, Breakdown of blood-brain and blood-spinal cord barriers during acute methamphetamine intoxication: role of brain temperature, CNS Neurol Disord Drug Targets 15 (9) (2016) 1129–1138.
[9] R. Harms, B. Morsey, C.W. Boyer, H.S. Fox, N. Sarvetnick, Methamphetamine administration targets multiple immune subsets and induces phenotypic alterations suggestive of immunosuppression, PLoS One 7 (12) (2012) e49897.
[10] L.R. Martinez, M.R. Mihu, A. Gacser, L. Santambrogio, J.D. Nosanchuk, Methamphetamine enhances histoplasmosis by immunosuppression of the host, J. Infect. Dis. 200 (1) (2009) 131–141.
[11] Z. Talloczy, J. Martinez, D. Joset, Y. Ray, A. Gacser, S. Toussi, N. Mizushima, J.D. Nosanchuk, H. Goldstein, J. Loike, D. Sulzer, L. Santambrogio, Methamphetamine inhibits antigen processing, presentation, and phagocytosis, PLoS Pathog. 4 (2) (2008) e28.

[12] M.R. Mihu, J. Roman-Sosa, A.K. Varshney, E.A. Eugenin, B.P. Shah, H. Ham Lee, L.N. Nguyen, A.J. Guimaraes, B.C. Fries, J.D. Nosanchuk, L.R. Martinez, Methamphetamine alters the antimicrobial efficacy of phagocytic cells during methicillin-resistant *Staphylococcus aureus* skin infection, MBio 6 (6) (2015) (e01622-15).
[13] W.J. Panenka, R.M. Procyshyn, T. Lecomte, G.W. MacEwan, S.W. Flynn, W.G. Honer, A.M. Barr, Methamphetamine use: a comprehensive review of molecular, preclinical and clinical findings, Drug Alcohol Depend. 129 (3) (2013) 167–179.
[14] W.P. Melega, A.K. Cho, D. Harvey, G. Lacan, Methamphetamine blood concentrations in human abusers: application to pharmacokinetic modeling, Synapse 61 (4) (2007) 216–220.
[15] E.A. Eugenin, J.M. Greco, S. Frases, J.D. Nosanchuk, L.R. Martinez, Methamphetamine alters blood brain barrier protein expression in mice, facilitating central nervous system infection by neurotropic *Cryptococcus neoformans*, J. Infect. Dis. 208 (4) (2013) 699–704.
[16] D. Patel, G.M. Desai, S. Frases, R.J. Cordero, C.M. DeLeon-Rodriguez, E.A. Eugenin, J.D. Nosanchuk, L.R. Martinez, Methamphetamine enhances *Cryptococcus neoformans* pulmonary infection and dissemination to the brain, MBio 4 (4) (2013).
[17] P.K. Thanos, R. Kim, F. Delis, M. Ananth, G. Chachati, M.J. Rocco, I. Masad, J.A. Muniz, S.C. Grant, M.S. Gold, J.L. Cadet, N.D. Volkow, Chronic methamphetamine effects on brain structure and function in rats, PLoS One 11 (6) (2016) e0155457.
[18] A. Shah, P.S. Silverstein, D.P. Singh, A. Kumar, Involvement of metabotropic glutamate receptor 5, AKT/PI3K signaling and NF-kappaB pathway in methamphetamine-mediated increase in IL-6 and IL-8 expression in astrocytes, J. Neuroinflammation 9 (2012) 52.
[19] X. Li, F. Wu, L. Xue, B. Wang, J. Li, Y. Chen, T. Chen, Methamphetamine causes neurotoxicity by promoting polarization of macrophages and inflammatory response, Hum Exp Toxicol 37 (5) (2018) 486–495.
[20] S.G. Fonseca, P.R. Romao, F. Figueiredo, R.H. Morais, H.C. Lima, S.H. Ferreira, F.Q. Cunha, TNF-alpha mediates the induction of nitric oxide synthase in macrophages but not in neutrophils in experimental cutaneous leishmaniasis, Eur. J. Immunol. 33 (8) (2003) 2297–2306.
[21] N. Imamura, H. Hida, N. Aihara, K. Ishida, Y. Kanda, H. Nishino, K. Yamada, Neurodegeneration of substantia nigra accompanied with macrophage/microglia infiltration after intrastriatal hemorrhage, Neurosci. Res. 46 (3) (2003) 289–298.
[22] Y. Takeshita, R.M. Ransohoff, Inflammatory cell trafficking across the blood-brain barrier: chemokine regulation and in vitro models, Immunol. Rev. 248 (1) (2012) 228–239.
[23] Y. Kobayashi, The role of chemokines in neutrophil biology, Front. Biosci. 13 (2008) 2400–2407.
[24] D. Vlahov, M. Sullivan, J. Astemborski, K.E. Nelson, Bacterial infections and skin cleaning prior to injection among intravenous drug users, Public Health Rep. 107 (5) (1992) 595–598.
[25] R.J. Gordon, F.D. Lowy, Bacterial infections in drug users, N. Engl. J. Med. 353 (18) (2005) 1945–1954.
[26] Y.T. Lai, Y.P. Tsai, C.G. Cherng, J.J. Ke, M.C. Ho, C.W. Tsai, L. Yu, Lipopolysaccharide mitagates methamphetamine-induced striatal dopamine depletion via modulating local TNF-alpha and dopamine transporter expression, J. Neural Transm. (Vienna) 116 (4) (2009) 405–415.
[27] B. Wang, T. Chen, J. Wang, Y. Jia, H. Ren, F. Wu, M. Hu, Y. Chen, Methamphetamine modulates the production of interleukin-6 and tumor necrosis factor-alpha via the cAMP/PKA/CREB signaling pathway in lipopolysaccharide-activated microglia, Int. Immunopharmacol. 56 (2018) 168–178.
[28] L.W. Fan, L.T. Tien, B. Zheng, Y. Pang, R.C. Lin, K.L. Simpson, T. Ma, P.G. Rhodes, Z. Cai, Dopaminergic neuronal injury in the adult rat brain following neonatal exposure to lipopolysaccharide and the silent neurotoxicity, Brain Behav. Immun. 25 (2) (2011) 286–297.
[29] J. Goncalves, T. Martins, R. Ferreira, N. Milhazes, F. Borges, C.F. Ribeiro, J.O. Malva, T.R. Macedo, A.P. Silva, Methamphetamine-induced early increase of IL-6 and TNF-alpha mRNA expression in the mouse brain, Ann. N. Y. Acad. Sci. 1139 (2008) (103-Highlights).